Design of crosslinked hybrid multilayer thin films from azido-functionalized polystyrenes and platinum nanoparticles

Samer Al Akhrass,[ab] François Gal,[b] Denis Damiron,[a] Pierre Alcouffe,[a] Craig J. Hawker,[c] Fabrice Cousin,[b] Géraldine Carrot[b] and Eric Drockenmuller*[a]

Received 11th August 2008, Accepted 23rd October 2008
First published as an Advance Article on the web 26th November 2008
DOI: 10.1039/b813928h

Crosslinked organic and hybrid multilayer thin films based on polystyrene-grafted platinum nanoparticles and azidomethyl-functionalized polystyrenes are built-up by sequential spin-coating and UV crosslinking processes. This approach allows to easily tune thickness, composition and periodicity of each layer, as highlighted by TEM and neutron reflectivity experiments. Room temperature UV crosslinking of hybrid layers allows to stabilize the layer prior to nanoparticles segregation.

Introduction

At every length scale, multilayer architectures and assemblies have been a wide source of inspiration in materials science. Among these, hybrid multilayer coatings including nanoparticles and polymer layers with a typical thickness of several nanometres, have attracted an increased interest not only for obtaining chemical and mechanical stability due to the polymer but also for inducing a wide range of interesting properties (*e.g.* electric, magnetic, catalytic, optical properties, *etc.*) due to the nanoparticles.[1] As a result, these tailored assemblies have significant potential in various applications such as microelectronics, catalysis, photonics, opto-electronics, functional coatings, membranes and photovoltaics.[2] The development of techniques controlling nanoparticle organization in thin films is an important aspect in applying their unique properties to reliable nanodevices.[3] Several methodologies such as Langmuir–Blodgett (LB) sequential depositions or electrostatic layer-by-layer (LbL) self-assembly can be employed to design well-defined organic and hybrid multilayer coatings.[4] While amenable to automation/manufacturing and extendable to a broad range of architectures, these techniques are primarily applied to the self-assembly of macromolecular amphiphilies or polyelectrolytes but remain rarely applied to nonpolar components. In addition, the range of thickness accessible using these techniques is limited to several nanometres per layer and due to their dynamic nature, the assemblies must be compatible with potential solvent or thermal treatments that may occur in specific applications. One strategy to overcome these issues is to adopt a spin-on strategy and to stabilize the multilayer thin films by crosslinking to prevent undesired film rearrangements such as dewetting, extensive swelling or dissolution, especially in thicker films.

As mentioned before, organic/inorganic hybrid materials are able to combine two or more desirable properties that can be tuned by particle size, shape and surface chemistry. The latter is crucial for the dispersion and stability of such functionalized nanoparticles in solutions, blends or thin films.[5] Moreover, it has been shown that polymer thin films could be stabilized from dewetting by the addition of dendrimers,[6] nanoparticles,[7] or by chemical crosslinking of the polymer matrix.[8,9] However, when exposing such hybrid films to solvents, high temperatures and magnetic or electrical fields, the nanoparticles can undergo aggregation or segregation to an interface.[10] The chemical modification of nanoparticle surfaces and tuning of the polymer matrix is therefore of special interest as it enables nanoparticle organization within the thin films to be controlled and directed.[11] Recently, a pioneering approach based on sequential spin-coating and annealing procedures has been developed by Mackay which allows the self-assembly of nonpolar linear polymers and nanoparticles into hybrid multilayer architectures with tunable film thickness to be fully realized using relatively simple and robust processing steps.[12] This approach relies on the thermal ring-opening of benzocyclobutene (BCB)-functionalized polymer chains, a crosslinking approach that has been previously applied to the crosslinking of nanoparticles and (diblock) copolymer thin films.[13] Indeed, a thin hybrid layer is spin-coated onto a solid substrate and then thermally annealed at 200–250 °C to activate crosslinking of the film. At the early stage of the annealing step, the initially dispersed nanoparticles segregate prior to complete crosslinking leading to the formation of a thin inorganic layer at the lower energy interface. However, the thickness of the inorganic layer is limited and depends on the quantity of inorganic nanoparticles in the spin-coating solution and the thickness of the resulting thin film. Therefore, designing robust, efficient and orthogonal procedures in order to elaborate and stabilize homogeneous hybrid multilayer thin films having a high content of nanoparticles is still a stimulating challenge.

Herein we describe a versatile method for the build-up of well-defined and tunable multilayer thin films based on the combination of polystyrene-grafted platinum (Pt) nanoparticles with

[a]*Laboratoire des Matériaux Polymères et Biomatériaux (UMR CNRS 5223), Université Claude Bernard Lyon 1, 15 Boulevard Latarjet, 69622 Villeurbanne, Cedex, France. E-mail: eric.drockenmuller@univ-lyon1.fr; Fax: +33 4 78 89 25 83; Tel: +33 4 72 43 15 67*
[b]*Laboratoire Léon Brillouin, CEA Saclay, 91191 Gif-sur-Yvette Cedex, France*
[c]*Departments of Materials, Chemistry and Biochemistry and Materials Research Laboratory, University of California, Santa Barbara, CA 93106–9510, USA*

photo-crosslinkable hydrido or deuterated azido-functionalized polystyrenes. This approach consists of straightforward and sequential spin-coating, UV irradiation and thermal annealing procedures which allow for an easy tuning of each layer thickness (h = 10–200 nm), composition (0–50 wt% of PS-grafted Pt nanoparticles) as well as a precise control of their registration and periodicity. Neutron reflectivity experiments performed on pure organic multilayers with alternated hydrido and deuterated layers provide an accurate characterization of layer thickness and of the limited interdiffusion occurring at each polymer/polymer interface in these multilayer architectures. The homogeneity of the resulting multilayer assemblies and the high level of dispersion for the PS-grafted Pt nanoparticles among hybrid layers have been confirmed by transmission electron microscopy (TEM). The presence of the grafted polystyrene chains overcomes the entropy driven segregation of the nanoparticles in the hybrid layer after spin-coating. In addition, a major benefit of this strategy is that UV crosslinking of the hybrid layers is performed at room temperature in the glassy state of PS which allows for the covalent stabilization of the polymer film prior to any annealing induced aggregation or interfacial segregation of the nanoparticles. This represents an efficient method for producing homogeneous hybrid multilayer architectures with tunable thickness and nanoparticle content.

Experimental

Synthesis of poly[styrene-*co*-(4-azidomethylstyrene)]

Crosslinkable azidomethyl-functionalized polystyrenes were obtained using a previously described procedure.[9] Briefly styrene or d_8-styrene and 4-chloromethyl styrene were copolymerized by NMRP. The resulting chloromethyl-functionalized random polystyrenes were converted to the corresponding azidomethyl-functionalized polystyrenes by NaN_3 in dimethylformamide. The contents of azide units were determined by ^{1}H NMR and found to be 17 mol% and 15 mol% for PSH and PSD, respectively.

Synthesis of polystyrene-grafted platinum nanoparticles

Initially, platinum nanoparticles having ATRP initiators at their surface were synthesized using previously reported ligand mediated technique and derivatization (over-grafting) reaction.[11,14] Subsequently, polystyrene chains were grown by "grafting-from" ATRP of styrene. Detailed synthesis and characterization procedures for these nanoparticles by small angle neutron scattering (SANS) and transmission electron microscopy (TEM) have been reported previously.[15] The polymerization from the 3 nm-core platinum particles has been carried out without the presence of free initiator. SANS has been carried out on these objects in deuterated toluene to match the contribution of the platinum core. The plot of scattering intensity versus wave vector shows a plateau at low q values and a decrease in q^{-2} in the intermediate range, similarly as observed in ref. 15 (data not shown). From the Guinier approximation, we could determine an overall radius of gyration of 10 nm. The number of polymer branches and their molecular weight could be deduced from the fit of the experimental curve with a star model.[15] We therefore found out that the number of chains per particle was seven and the weight-average molecular weight 50 kDa. This represents a weight fraction of polymers (as determined by thermogravimetric analysis) of 87%.

Preparation of (hybrid) multilayer thin films

Each layer of the multilayer assemblies was obtained by spin-coating a dilute toluene solution (*ca.* 10 mg mL^{-1}) of PSH (or PSD) with or without polystyrene-grafted platinum nanoparticles onto a polished silicon wafer (diameter: 2 inches, thickness: 2000 ± 25 μm, orientation: 100). The weight fraction of grafted nanoparticles in the grafting solution was varied from 20 to 50 wt%. After spin-coating, the thin films were crosslinked by UV curing (VL-115, λ = 365 nm, 1 mW cm^{-2}, distance between sample and UV lamp ~5 cm) for 1 h followed by two hours of annealing at 180 °C. This was repeated ***n*** times to afford a (hybrid) multilayer assembly having ***n*** distinct crosslinked layers.

Neutron reflectivity measurements

The neutron reflectivity measurements were performed on the time-of-flight reflectometer EROS at LLB (CEA, Saclay). During the experiment, we use all the wavelengths λ provided by the neutron source from 3 to 25 Å with a constant $\Delta\lambda/\lambda$ of 0.11. For each sample three angles (θ = 0.93°, 1.62° and 3.00°) with a $\Delta\theta$ of 0.05° were used to get a q range of 0.07 Å^{-1} < Q < 0.2 Å^{-1}. The experimental resolution was taken into account in the fitting procedure.

Transmission electron microscopy experiments

The TEM experiments were performed at the "Centre Technologique des Microstructures" of the University Claude Bernard Lyon1 using a Philips CM120 transmission electron microscope and an acceleration voltage of 80 KV. Samples for top view imaging of single PSH/PtH hybrid layers were prepared by floating the crosslinked network from a glass substrate onto the surface of distilled water and subsequent deposition onto a copper grid. For cross-section imaging of hybrid multilayer architectures, samples were prepared as described in Scheme 2 using a glass substrate. The multilayer thin-film was floated onto the surface of distilled water, collected with a polyolefin substrate (Thermanox, Delta microscopies, France), dried and included in an epoxy resin after sputtering a thin layer of gold in order to facilitate the determination of the air/polymer interface. TEM samples were then microtomed using an ultramicrotom (LEICA) to obtain normal sections *ca.* 50 nm thick that were transferred onto a copper grid.

Results and discussion

Materials and process for crosslinked multilayer assemblies

The build-up of well-defined hybrid multilayer thin films by sequential spin-coating procedures requires accurate control of functionality, thickness and stability of each consecutive layer. As a result, in addition to a rational choice for the nature of the polymer, nanoparticle and polymeric shell, an efficient crosslinking method is crucial to prevent dissolution and to minimize interdiffusion of the layers during the spin-coating and annealing steps. Photochemical crosslinking of azidomethyl substituted polymers has previously been employed for obtaining photodefinable crosslinked underlayers for the controlled orientation

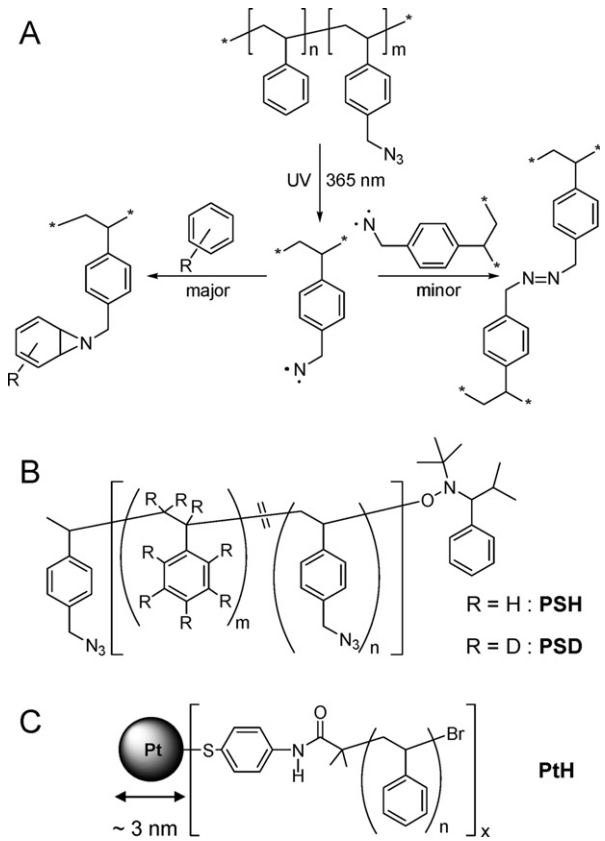

Scheme 1 (A) Photochemical crosslinking principle of azidomethyl-functionalized polystyrenes, (B) hydrido (PSH) and deuterated (PSD) azidomethyl-functionalized random polystyrenes, (C) hydrido polystyrene-grafted platinum nanoparticles (PtH).

of diblock copolymers as well as for preventing the dewetting of polystyrene thin films.[9,16] Scheme 1A shows the main crosslinking pathways occurring during UV irradiation of benzylazides, leading to aziridine (major) and diazo (minor) covalent crosslinks after the initial formation of transient nitrene radicals. An important aspect of this crosslinking pathway is that the only by-product released is nitrogen (N_2) and there is no need to use additional crosslinking agents (*e.g.* initiators, monomers, catalysts…) which significantly simplifies the procedure and removes any additional components from the resulting network which may disturb further analysis or treatment. The presence of such heterogeneities has been shown to increase the interfacial width between two polymer layers.[17]

Tailor-made hydrido (PSH) and deuterated (PSD) random copolymers of *p*-azidomethylstyrene and styrene or d_8-styrene (Scheme 1B) were synthesized using previously described nitroxide mediated radical polymerization (NMRP) and post-azidation chemical modification procedures.[9] Both derivatives have a weight average molar mass (M_w) of *ca.* 130 kDa and polydispersity indices (*PDI*) of 1.65, with 17 mol% and 15 mol% of *p*-azidomethylstyrene units for PSH and PSD, respectively. Hydrido PS-grafted platinum nanoparticles (PtH, Scheme 1C) were synthesized in two steps by initiator-derivatization of platinum nanoparticles followed by "grafting-from" atom transfer radical polymerization (ATRP) of styrene.[15] The platinum core has an average diameter of *ca.* 3 nm and is surrounded by PS chains (weight fraction of 87%) with the radius of gyration for the core-shell nanoparticle being 10 nm as determined using small-angle neutron scattering (SANS). The fit of the SANS spectrum obtained using a star model gives an average of seven polystyrene chains per nanoparticle having a M_w of *ca.* 50 kDa.[15] It must be pointed out that UV crosslinking of the azidomethyl-functionalized polystyrene also induces the covalent anchorage of the PS-grafted nanoparticles to the resulting polymer network.

The process used for the elaboration of crosslinked (hybrid) multilayer thin films is described in Scheme 2. After spin-coating of the polymer from a toluene solution (that can also include PS-grafted Pt nanoparticles) the resulting (hybrid) thin film is crosslinked by UV irradiation (1 h @ 365 nm). The film is then annealed at 180 °C for 2 h in order to improve the crosslinking by reopening the potentially formed diazo linkages and to relax the residual stresses generally observed in spin-coated thin films,[9,18] however no changes in nanoparticle distribution or position is observed during the annealing step. Repeating the procedure described above (spin-coating, UV curing and thermal annealing) ***n*** times affords well-defined (hybrid) multilayer architectures having ***n*** distinct layers. The sequence, the thickness and the composition of each layer is easily adjusted by varying the weight fraction and nature of the materials in the spin-casting solution leading to a versatile simple and robust process.

Neutron reflectivity of H/D organic multilayers

In order to probe the efficiency of this process for fabricating tunable polymer multilayers with limited interdiffusion, the dimensions of organic multilayer assemblies without PS-grafted Pt nanoparticles and consisting of alternating hydrido and deuterated crosslinked layers were first investigated in detail by neutron reflectivity. This technique allows each layer thickness to be precisely determined and the interfacial width between each polymer/polymer interfaces to be probed. The reflectivity curves for multilayers alternating up to three crosslinked PSH/PSD bilayers on silicon wafers are presented in Fig. 1. Fig. 1B presents the curve in a RQ^4 *vs.* Q which allows greater insight into the multilayer structure since it compensates the Q^{-4} decay of the pure Si/air interface. Samples (i–iii) correspond to assemblies of 2, 4 and 6 layers respectively, with thicknesses varying from 130

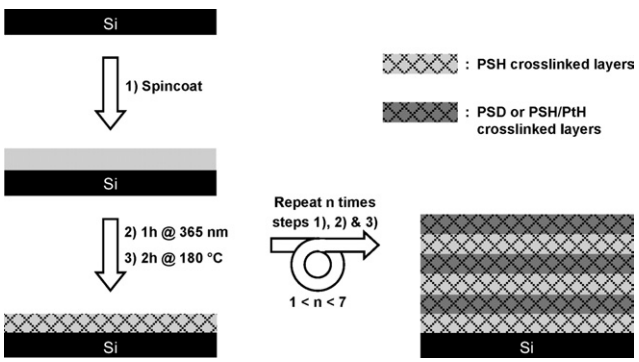

Scheme 2 Sequential elaboration of crosslinked organic and hybrid multilayer thin-films.

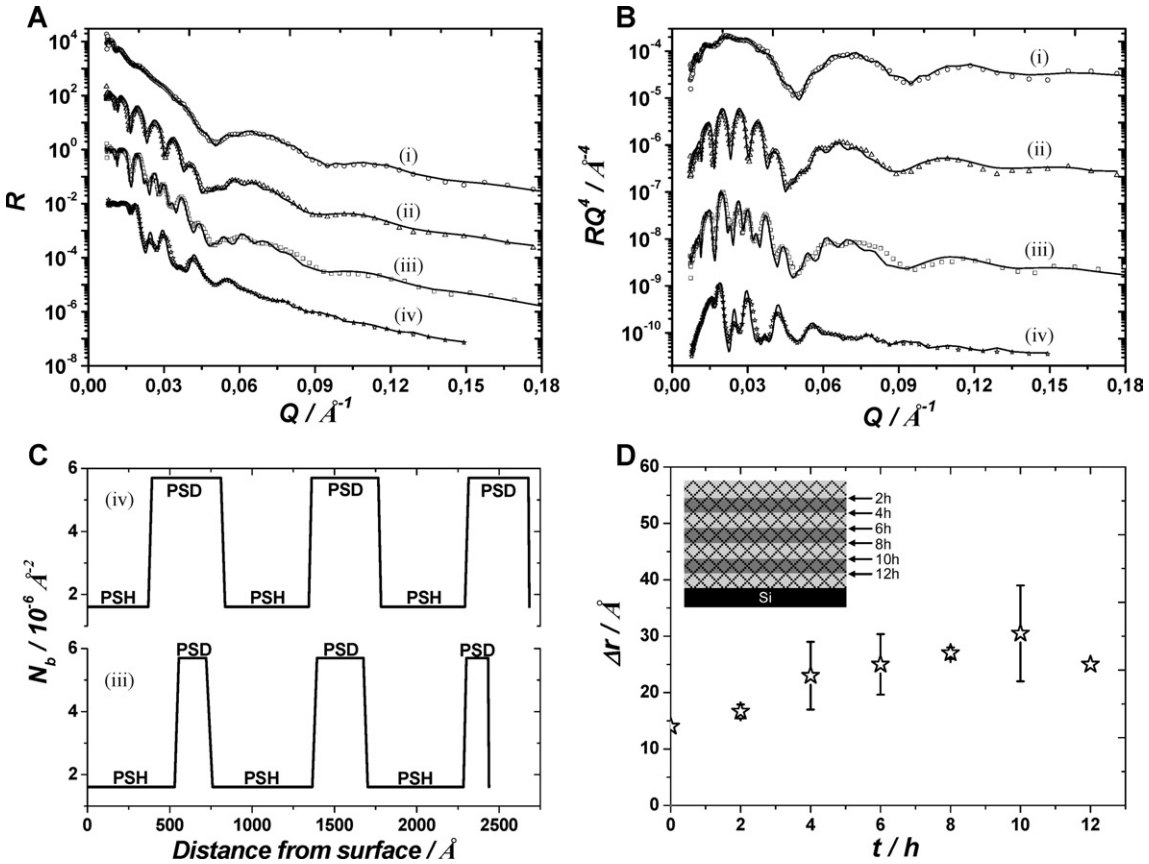

Fig. 1 (A) Reflectivity (R) *vs.* the scattering vector (Q) and (B) RQ^4 *vs.* Q for PSH/PSD multilayer thin films on silicon wafers. Curves (i–iii) correspond respectively to 2, 4 and 6 layers assemblies with thicknesses varying from 13 to 28 nm for PSD and 53 to 64 nm for PSH. Curve (iv) corresponds to an assembly of 6 layers with similar thickness for PSH and thicker layers of PSD (*ca.* 39–44 nm). The solid lines represent the best fits for each data. The thickness (h) of each layer and interfacial width (Δr) of each PSH/PSD interface are reported in Table 1. (C) Neutron density length (N_b) profiles for PSH/PSD multilayers (iii) and (iv). (D) Interfacial width (Δr) *vs.* annealing time at 180 °C resulting from neutron reflectivity experiments on a seven layer PSH/PSD assembly. Δr at t = 0 corresponds to the interfacial width of a polymer/polymer interface before annealing.

to 280 Å for the PSD layers and from 530 to 640 Å for the PSH layers. Sample (iv) represents an assembly of 6 layers with thicknesses from 390 to 440 Å for the PSD layers and from 370 to 530 Å for the PSH layers. All curves have been fitted by minimizing the least squares χ^2 between experimental curves and reflectivity curves calculated by the standard optical matrix method. A multilayer model was used that includes the SiO_2 layer (6 Å) at the surface of silicon with a neutron density length (N_b) of 3.41×10^{-6} Å^{-2}, crosslinked PSH layers with a N_b of 1.61×10^{-6} Å^{-2}, and crosslinked PSD layers with a N_b of 5.70×10^{-6} Å^{-2}. The N_b values were determined experimentally from neutron reflectivity experiments performed on corresponding single layers. They are different than those obtained for pure hydrido and deuterated polystyrenes ($N_b = 1.41 \times 10^{-6}$ Å^{-2} and 6.38×10^{-6} Å^{-2}, respectively). Indeed, the presence of 17 mol% of azide groups increases the N_b of PSH while incorporation of 15 mol% of hydrogenated *p*-azidomethylstyrene units decreases the N_b of PSD. Nevertheless, the large neutronic contrast between the PSD and PSH layers allows an accurate determination of each layer thickness as well as the interfacial roughness which is

Table 1 Thickness (h) and interfacial roughness (Δr) of multilayer assemblies (i–iv) obtained from the best fits of the reflectivity curves in Fig. 1A and B. The average scattering length densities (N_b) of PSH and PSD layers were calculated as 1.61×10^{-6} Å^{-2} and 5.70×10^{-6} Å^{-2}, respectively

		(i)		(ii)		(iii)		(iv)	
Layer	N°	h/Å	Δr/Å	h/Å	Δr/Å	h/Å	Δr/Å	h/Å	Δr/Å
1	PSH	577	15	636	31	530	25	370	22
2	PSD	135	4	183	29	166	39	440	26
3	PSH	—	—	640	17	606	28	534	18
4	PSD	—	—	143	5	282	26	422	17
5	PSH	—	—	—	—	581	18	526	23
6	PSD	—	—	—	—	132	6	386	5

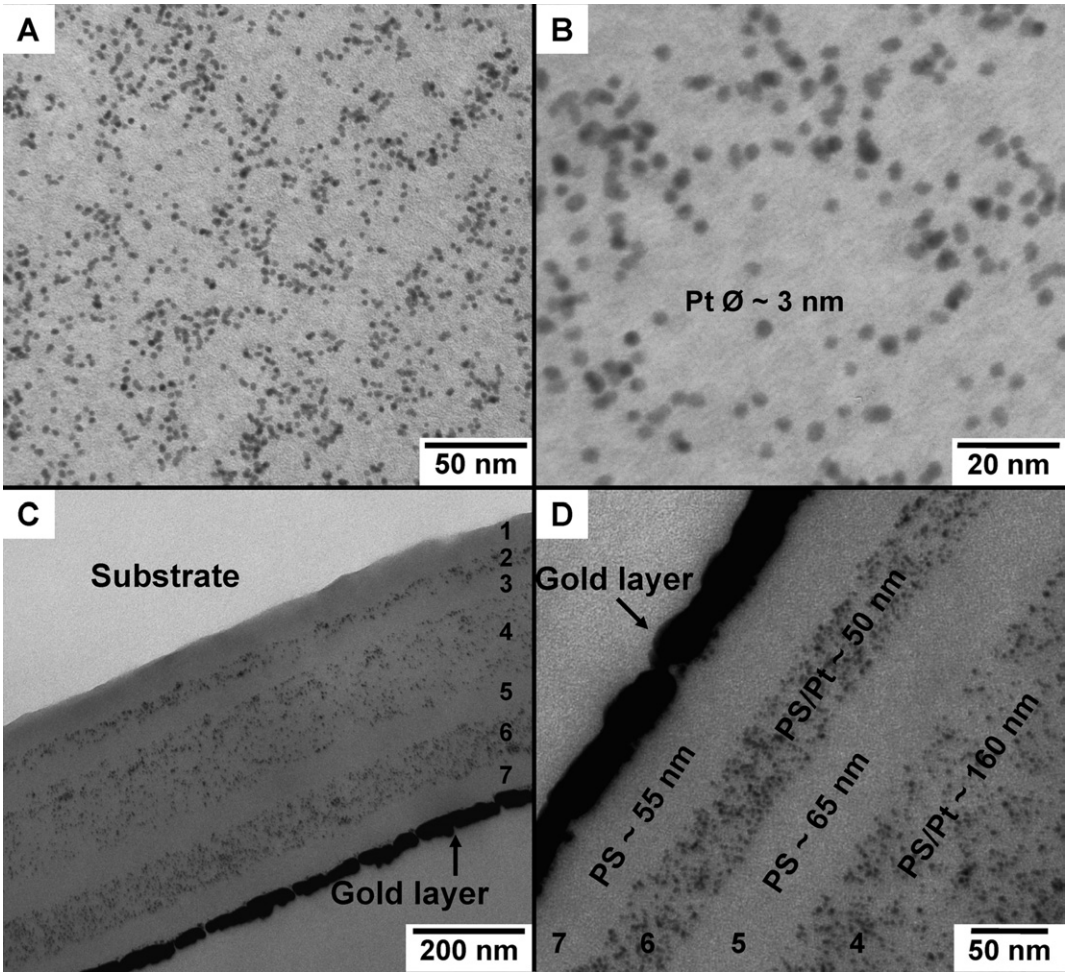

Fig. 2 (A and B) top view TEM images of a floated single PSH/PtH hybrid crosslinked layer ($h = 30$ nm and PtH = 20 wt%). (C and D) Cross-sectional TEM images of a 7 layer hybrid multilayer assembly with varying layers thickness and a PtH content of 50 wt%.

directly related to the interdiffusion occurring at PSH/PSD interfaces. Results from the best fits of reflectivity curves are listed in Table 1 and show the average thickness (h) of each individual layer and the average roughness (Δr) of each polymer/polymer interface. First, the low values obtained for polymer/polymer interfacial roughness ($\Delta r < 40$ Å) are independent of the film thickness and confirm the efficiency of the crosslinking process. Also, the roughness of the air/polymer interface ($\Delta r \sim 5$ Å) is even lower and the difference compared to sandwiched layers is directly related to the interdiffusion resulting from the spin-coating and annealing steps. It must be noted that these values are significantly lower than the diameter of a random coil (radius of gyration of a 130 kDa PS is *ca.* 100 Å).

In addition, Fig. 1C presents the N_b profiles for samples (iii) and (iv) consisting of three alternating PSH/PSD bilayers with varying thicknesses. These profiles show the robustness and the reliability of the overall multilayer assemblies and is characterized by sharp interfaces and high contrast between consecutive layers. To further characterize these multilayer structures and to understand the role of interdiffusion at polymer/polymer interfaces, the evolution of interfacial width (Δr) between two adjacent crosslinked layers with annealing time was monitored. This evolution can be extracted from data such as those presented in Table 1, as for each multilayer system the layer *n-1* has been annealed two hours more than the layer *n*. Therefore we can consider that the first polymer/polymer interface of a seven layer system has been annealed 6 × 2 h, whereas the seventh layer (or the 6th polymer/polymer interface) has been annealed for only 2 h. Based on this, Fig. 1D represents the evolution of Δr as a function of annealing time. First, it can be noticed that an increase of Δr from 5 Å (for the air/polymer interface of each of the multilayer assemblies in Table 1) to 15 Å (for a polymer/polymer interface before annealing) is observed, this being directly related to the interdiffusion resulting from the spin-coating process. Then, Δr increases with time as a result of subsequent polymer interdiffusion at elevated temperature. Interfacial roughness is initially induced by spin-casting and, as usually observed, if solvent remains trapped in the crosslinked layer then both networks may swell each other,[17,19] which leads to a small degree of interpenetration across the interface. Therefore, dangling chain ends in the polymer network are able to stretch and interpenetrate the opposite side of the interface. The maximal value of Δr reached after *ca.* 4 h is comparable with twice the distance of the maximal length of the dangling chains at the polymer/polymer interface. For the crosslinking density studied herein, this means that the maximal length is 12 Å

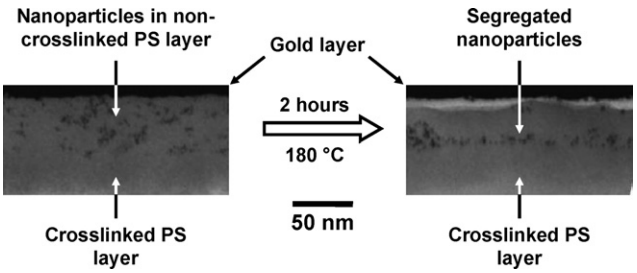

Fig. 3 Cross-sectional TEM images of a mixed layer of PtH and non-functionalized polystyrene deposited over a layer of crosslinked PSH: (A) before and (B) after annealing two hours at 180 °C.

(~1 crosslink every 6 monomers as the content of azide units is ~15 mol%) which gives an estimation of Δr ~25 Å, a value close to the experimental interfacial roughness determined from Fig. 1D. The extent of interpenetration between two consecutive networks can therefore be tuned by the crosslinking density.

TEM of hybrid multilayers containing platinum nanoparticles

Neutron reflectivity confirmed the high level of control during the fabrication of these PSH/PSD crosslinked multilayers and their associated stability. The versatility of this approach was then examined by the elaboration and characterization of hybrid multilayers comprised of alternating PSH and PSH/PtH films. The first challenge in this design is to generate and stabilize hybrid PSH/PtH single layers. Initially these layers were formed by the processing of platinum nanoparticles without polymer branches (Pt nanoparticles functionalized with alkylated ligands) but repeated experiments resulted in the formation of heterogeneous hybrid layers and aggregated nanoparticles. To overcome this issue and to obtain homogeneous hybrid thin films, PS chains were grafted to the surface of the platinum nanoparticle which not only allows excellent dissolution in toluene solutions but also a homogeneous dispersion of the nanoparticles in the hybrid layer after spin-coating. Secondly, the PS branches can participate in the crosslinking process, yielding nanoparticles covalently linked to the polymer network. Therefore a single hybrid layer of *ca.* 50 nm and 20 wt% of PtH was spin-coated onto a glass substrate, crosslinked, floated and characterized by a top view TEM image in order to visualize the nanoparticles distribution in the volume of the polymer matrix. Fig. 2A and B highlight the uniform distribution of the PS-grafted Pt nanoparticles in the hybrid layer after the crosslinking process. The nanoparticles are homogeneously distributed and the apparent contact between a small percentage of nanoparticles is most likely due to the top view image, leading to superposition. However, the image does clearly show that the 3D organization and dispersion of the nanoparticles remains after the annealing step.

Once the homogeneous PtH nanoparticles distribution among a single hybrid layer was confirmed, the fidelity of the overall hybrid multilayer assemblies was investigated by TEM. A seven layer hybrid assembly was therefore constructed on a glass substrate and the cross-section views of the assembly analyzed by TEM. To demonstrate the tunable character of this process, the thickness of each layer (30–160 nm) as well as the nanoparticle content inside hybrid layers (20–50 wt% of PtH nanoparticles) were varied. Fig. 2C and D represent two magnifications of a cross-section TEM micrograph obtained for a multilayer assembly of hybrid layers (layers 2, 4 and 6) with thicknesses of *ca.* 35 nm, 160 nm and 50 nm, respectively, alternated with crosslinked PSH layers (layers 1, 3, 5 and 7) with thicknesses of *ca.* 60 nm, 45 nm, 65 nm and 55 nm, respectively. Corroborating neutron reflectivity results, the TEM images show a well defined hybrid multilayer architecture with relatively low interdiffusion between layers which is independent of composition, thickness and number of layers. Moreover, Fig. 2D shows a uniform dispersion of Pt nanoparticles in the volume of the hybrid layers without any significant aggregation or segregation to interfaces.

Additional TEM experiments were performed on a bilayer hybrid system in order to investigate if the absence of nanoparticles segregation is due to the crosslinking process and/or to the nanoparticle dispersion by the PS branches. For this, a *ca.* 50 nm hybrid layer consisting of 20 wt% of PtH and a non-functionalized linear polystyrene was deposited over a *ca.* 40 nm crosslinked layer of PSH. Two different samples with and without 2 hours of annealing at 180 °C were analyzed by TEM with cross-sectional images of the bilayer before annealing (Fig. 3A) showing a homogeneous dispersion of the nanoparticles in the PS film and a sharp interface between the PSH and the non-crosslinked hybrid layer. However, after annealing (Fig. 3B) we observe a segregation of the polymer-grafted nanoparticles which accumulate at the interface between crosslinked and non crosslinked PS layers. This entropically driven segregation is in agreement with the previously reported observation on hybrid thin films.[11,20] Thus, even if PS branches minimize the entropic forces responsible for nanoparticles segregation prior to crosslinking, the nanoparticles segregate when hybrid films are annealed at 180 °C. Therefore while PS branches favor nanoparticles solubilization and dispersion in the polymer matrix, this effect cannot prevent the migration of the PS-grafted nanoparticles induced by heat. From these studies it can be concluded that crosslinking of the matrix and possible incorporation of the nanoparticles through their branches in the polymeric network is necessary to obtain stable dispersion within the multilayer. However, it must be noticed that in Fig. 3B nanoparticles remain at the interface with the PSH crosslinked layer which acts as an entropic barrier to their further migration to the substrate or other interfaces.

Conclusions

In conclusion, the PS-grafted platinum nanoparticle/azidomethyl-functionalized polystyrene model system studied herein represents a powerful method for the versatile and robust elaboration of (hybrid) multilayer architectures and their stabilization by UV crosslinking. The highly modular nature of this process allows accurate control over the 3D organization of nanoparticles embedded into a 2D arrangement of polymer layers which is extendable to different types of substrates, nanoparticles, and polymers. These novel nanoscale systems have the potential to lead to a wide range of properties and applications in materials science and nanotechnology.

Acknowledgements

Authors gratefully acknowledge the financial supports from the Agence Nationale de la Recherche under contract

ANR-07-JCJC-0020-01, the European Community's "Marie-Curie Actions" under contract MRTN-CT-2004-504052 and the NSF [CHE-0514031 and the MRSEC Program DMR-0520415 (MRL-UCSB)].

References

1 J. Schmitt, G. Decher, W. J. Dressik, S. L. Brandow, R. E. Geer, R. Shashidar and J. M. Calvert, *Adv. Mater.*, 1997, **9**, 61; R. Davies, G. A. Schurr, P. Meenan, R. D. Nelson, H. E. Bergna, C. A. S. Brevett and R. H. Goldbaum, *Adv. Mater.*, 1998, **10**, 1264; P. T. Hamond, *Adv. Mater.*, 2004, **16**, 1271; G. Decher and J. Schlenoff, in *Applications of LbL Multilayer Thin Films: Sequential Assembly of Nanocomposite Materials*, ed. H. Baltes, W. Göpel and J. Hesse, Wiley-VCH, Weinheim, 2003, vol. 2, (ch. 2).

2 L. Richert, F. Boulmedais, P. Lavalle, J. Mutterer, E. Ferreux, G. Decher, P. Schaaf, J.-C. Voegel and C. Picart, *Biomacromolecules*, 2004, **5**, 284; H. Liao, W. Lu, S. Yu, W. Wen and G. K. L. Wong, *J. Opt. Soc. Am. B*, 2005, **22**, 1923; C.-J. Zhong and M. M. Maye, *Adv. Mater.*, 2001, **13**, 1507.

3 M. P. Pinelli, *J. Phys. Chem. B*, 2001, **105**, 3358.

4 E. R. Kleinfeld and G. S. Ferguson, *Chem. Mater.*, 1996, **8**, 1575; N. A. Kotov, T. Haraszti, L. Turi, G. Zavala, R. E. Geer, I. Dekany and J. H. Fendler, *J. Am. Chem. Soc.*, 1997, **119**, 6821; G. Decher, *Science*, 1997, **277**, 1232; J.-A. He, L. Samuelson, L. Li, J. Kumar and S. K. Tripathy, *Langmuir*, 1998, **14**, 1674; X. Fan, J. Locklin, J. H. Youk, W. Blanton, C. Xiav and R. Advincula, *Chem. Mater.*, 2002, **14**, 2184; J. Dai and M. L. Bruening, *Nano Lett.*, 2002, **2**, 497; S. Parvin, J. Matsui, E. Sato and T. J. Miyashita, *Coll. Int. Sci.*, 2007, **313**, 128.

5 A. P. Alivisatos, *Science*, 1996, **271**, 933; S. J. Olddenburg, R. D. Averitt, S. L. Westcott and N. J. Halas, *Chem. Phys. Lett.*, 1998, **288**, 243; A. Henglein, *Langmuir*, 1999, **15**, 6738; M. D. Malinsky, K. L. Kelly, G. C. Schatz and R. P. Van Duyne, *J. Am. Chem. Soc.*, 2001, **123**, 1471; C. J. Murphy and N. R. Jana, *Adv. Mater.*, 2002, **14**, 80; W. Cheng, S. Dong and E. Wang, *J. Phys. Chem. B*, 2004, **108**, 19146; R. Matsuno, H. Otsuka and A. Takahara, *Soft Matter*, 2006, **2**, 415; J. Oberdisse, *Soft Matter*, 2006, **2**, 29.

6 M. E. Mackay, Y. Hong, M. Jeong, S. Hong, T. P. Russell, C. J. Hawker, R. Vestberg and J. F. Douglas, *Langmuir*, 2002, **18**, 1877.

7 K. A. Barnes, A. Karim, J. F. Douglas, A. I. Nakatani, H. Gruell and E. J. Amis, *Macromolecules*, 2000, **33**, 4177; R. S. Krishnan, M. E. Mackay, C. J. Hawker and B. Van Horn, *Langmuir*, 2005, **21**, 5770.

8 G. T. Carroll, M. E. Sojka, X. Lei, N. J. Turro and J. T. Koberstein, *Langmuir*, 2006, **22**, 7748.

9 S. Al Akhrass, R.-V. Ostaci, Y. Grohens, E. Drockenmuller and G. Reiter, *Langmuir*, 2008, **24**, 1884.

10 S. Gupta, Q. L. Zhang, T. Emrick, A. C. Balazs and T. P. Russell, *Nat. Mater.*, 2006, **5**, 229; M. Stamm and J.-U. Sommer, *Nat. Mater.*, 2007, **6**, 260.

11 A. El Harrak, G. Carrot, J. Oberdisse and F. Boué, *Macromolecules*, 2004, **37**, 6376; A. El Harrak, G. Carrot, J. Oberdisse and F. Boué, *Polymer*, 2005, **46**, 1095; G. Carrot, A. El Harrak, J. Oberdisse, J. Jestin and F. Boue, *Soft Matter*, 2006, **2**, 1043; C. B. Bailly, A.-C. Donnenwirth, C. Bartholome, E. Beyou and E. Bourgeat-Lami, *J. Nanomaterials*, 2006, 1.

12 R. S. Krishnan, M. E. Mackay, P. M. Duxbury, A. Pastor, C. J. Hawker, B. Van Horn, S. Asokan and M. S. Wong, *Nano Lett.*, 2007, **7**, 484.

13 D. Y. Ryu, K. Shin, E. Drockenmuller, C. J. Hawker and T. P. Russell, *Science*, 2005, **308**, 236; E. Drockenmuller, L. Y. T. Li, E. Harth, T. P. Russell, H. C. Kim and C. J. Hawker, *J. Polym. Sci. Part A: Polym. Chem.*, 2005, **43**, 1028; T. E. Dukette, M. E. Mackay, B. Van Horn, K. L. Wooley, E. Drockenmuller, M. Malkoch and C. J. Hawker, *Nanoletters*, 2005, **5**, 1704; J. M. Leiston-Belanger, T. P. Russell, E. Drockenmuller and C. J. Hawker, *Macromolecules*, 2005, **38**, 7676; D. Y. Ryu, J.-Y. Wang, K. A. Lavery, E. Drockenmuller, S. K. Satija, C. J. Hawker and T. P. Russell, *Macromolecules*, 2007, **40**, 4296; B. Ma, F. Lauterwasser, L. Deng, C. S. Zonte, B. J. Kim, J. M. J. Frechet, C. Borek and M. E. Thompson, *Chem. Mater.*, 2007, **19**, 4827; E. Kim, C. Shin, H. Ahn, D. Y. Ryu, J. Bang, C. J. Hawker and T. P. Russell, *Soft Matter*, 2008, **4**, 475.

14 H. Perez, R. M. Lisboa de Sousa, J.-P. Pradeau and P.-A. Albouy, *Chem. Mater.*, 2001, **13**, 1512.

15 G. Carrot and H. Perez, *Polym. Prep.*, 2006, 827; G. Carrot, F. Gal, J. Vinas and H. Perez, *Langmuir*, DOI: 10.1021/la802862q.

16 J. Bang, J. Bae, P. Löwenhielm, C. Spiessberger, S. A. Given-Beck, T. P. Russell and C. J. Hawker, *Adv. Mater.*, 2007, **19**, 4552.

17 M. Geoghegan, F. Boué, G. Bacri, A. Menelle and D. G. Bucknall, *Eur. Phys. J. B*, 1998, **3**, 83; J. Lal, J. Bastide, R. Bansil and F. Boué, *Macromolecules*, 1993, **26**, 6092.

18 G. Reiter, M. Hamieh, P. Damman, S. Sclavons, S. Gabriele, T. Vilmin and E. Raphael, *Nat. Mater.*, 2005, **4**, 754; M. H. Yang, S. Y. Hou, Y. L. Chang and A. C.-M. Yang, *Phys. Rev. Lett.*, 2006, **96**, 066105; P. Damman, S. Gabriele, S. Sclavons, S. Desprez, D. Villers, T. Vilmin, E. Raphael, M. Hamieh, S. Al Akhrass and G. Reiter, *Phys. Rev. Lett.*, 2007, **99**, 036101; S. Al Akhrass, G. Reiter, S. Y. Hou, M. H. Yang, Y. L. Chang, F. C. Chang, C. F. Wang and A. C.-M. Yang, *Phys. Rev. Lett.*, 2008, **100**, 178301.

19 F. Brochard, *J. Phys. France*, 1981, **42**, 505.

20 Y. Lin, H. Skaff, T. Emrick, A. D. Dinsmore and T. P. Russell, *Science*, 2003, **299**, 226; R. S. Krishnan, M. E. Mackay, P. M. Duxbury, C. J. Hawker, S. Asokan, M. S. Wong, R. Goyette and P. Thiyagarajan, *J. Phys.: Condens. Matter*, 2007, **19**, 356003; E. S. McGarrity, A. L. Frischknecht, L. J. D. Frink and M. E. Mackay, *Phys. Rev. Lett.*, 2007, **99**, 238302; M. E. Mackay, A. Tuteja, P. M. Duxbury, C. J. Hawker, B. Van Horn, Z. Guan, G. Chen and R. S. Krishnan, *Science*, 2006, **311**, 1740.

